

# Comparison of moduli determined by DMT and backfigured from local strain measurements under a 40 m diameter circular test load in the Venice area

S. Marchetti, P. Monaco, M. Calabrese & G. Totani  
*University of L'Aquila, Italy*

Keywords: Flat dilatometer test, constrained modulus, stiffness decay curves, test embankment, Venice

**ABSTRACT:** A full-scale instrumented test embankment (40 m diameter, 6.7 m height, applied load 104 kPa) was constructed at the site of Treporti, typical of the highly stratified, predominantly silty deposits of the Venice lagoon. DMT results at Treporti and comparisons of DMT-predicted vs measured settlements, indicating good agreement, have been presented by Marchetti et al. (2004). This paper concentrates mainly on the comparison of moduli obtained by DMT and from back-analysis of the test embankment performance. The moduli comparisons were carried out not only when the load was fully applied, but also at various stages during loading. In this way it was possible to reconstruct the in situ curves of decay of soil stiffness with strain level. Such curves were backfigured from vertical strains measured at 1 m depth intervals under the increasing loads throughout the embankment construction. The comparison of these curves with datapoints corresponding to DMT constrained moduli ( $M_{DMT}$ ) indicates that  $M_{DMT}$  can be possibly associated to a strain range  $\epsilon_v \approx 0.1$  to 1 %, 0.5 % on average. This finding may help for the development of methods for deriving in situ decay curves of soil stiffness with strain level from seismic dilatometer (SDMT).

## 1 INTRODUCTION

A full-scale instrumented test embankment was recently constructed at the site of Treporti (Venice, Italy) as part of a research project aimed at the characterization/modeling of the Venetian soils, in connection with plans for the protection of Venice and its lagoon against recurrent flooding.

The construction of the sand embankment, of cylindrical shape (40 m diameter) with geogrid-reinforced vertical walls, started on 12 September 2002 and ended on 10 March 2003. It was carried out in 13 steps by placing sand layers of 0.50 m thickness each. When completed, the sand embankment was covered with 0.20 m of gravel, thus reaching a final height of 6.70 m and a load of 104 kPa.

The embankment was heavily instrumented, at the surface and down to 60 m depth, for monitoring total settlements, local vertical strains, pore pressures and horizontal deformations. Data records of measurements are available so far over a period of more than two years after the beginning of the embankment construction.

The site of Treporti, typical of the Venice lagoon, has been carefully characterized by means of numerous in situ and laboratory tests, performed by various research groups.

Relevant results from the research program at Treporti have already been published (Simonini 2004, Marchetti et al. 2004, McGillivray & Mayne 2004, Gottardi & Tonni 2004, 2005, Cola & Simonini 2005).

Results of flat dilatometer tests (DMT) carried out at Treporti were presented by Marchetti et al. (2004), as well as comparisons of settlements predicted by DMT – before the field measurements were available – and measured. The settlement predicted by DMT at the end of construction (net of secondary developed during construction) was found in good agreement with the observed settlement.

This paper concentrates mainly on the comparison of moduli obtained from DMT and from back-analysis of the test embankment performance.

Also shown in this paper are in situ decay curves of soil stiffness with strain level backfigured from vertical strains measured at 1 m depth intervals under various loads throughout the embankment construction. Datapoints corresponding to the DMT constrained moduli ( $M_{DMT}$ ) are superimposed to the observed decay curves, in order to locate the strain range associated to  $M_{DMT}$ , in view of the possible development of methods for deriving in situ decay curves of soil stiffness with strain level from the seismic dilatometer (SDMT).

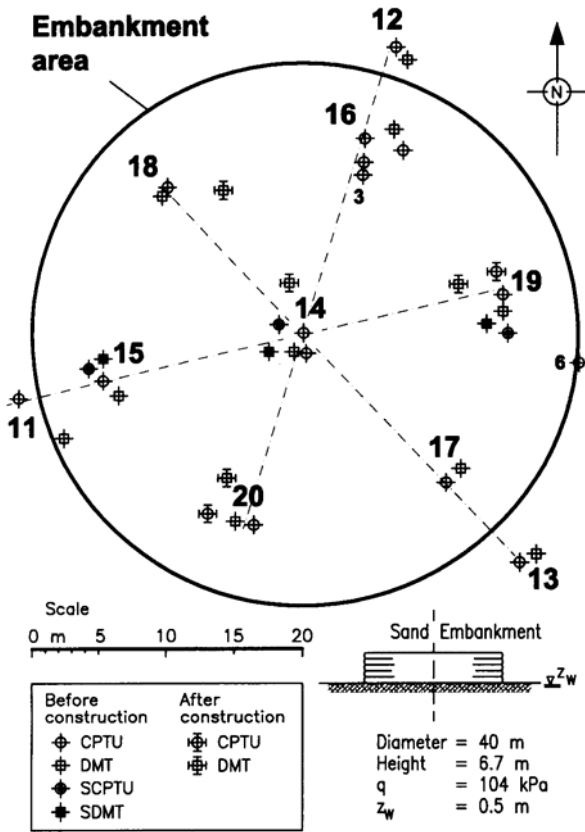


Fig. 1. Treporti test embankment and location of in situ tests

## 2 BASIC PROPERTIES OF THE VENETIAN SOILS

The soil deposits in the Venice lagoon are composed of a complex system of interbedded sands, silts and silty clays with inclusions of peat. Due to their complex geological history (Ricceri & Butterfield 1974), the sediments exhibit great non-homogeneity even in the horizontal direction. On the other hand, such non-homogeneities, seen on a larger scale, repeat themselves rather "uniformly" (see Fig. 3 later in the paper).

The main characteristic of the Venice lagoon soils is the presence of a predominant silt fraction combined with clay and/or sand, forming a chaotic interbedding of different sediments, whose basic mineralogy varies narrowly, as a result of a unique geological origin and a common depositional environment (Simonini 2004).

The cohesive layers are predominantly silts and very silty clays (ML and CL of the Unified Soil Classification System) of low plasticity. Granular layers are mainly composed of medium-fine sands and fine silty sands (SP-SM). Some thin peat layers are found embedded in the soil profile.

## 3 SITE INVESTIGATION AT TREPOTI

The site of Treporti was extensively investigated before the embankment construction by means of flat

dilatometer tests (DMT), piezocone tests (CPTU), seismic dilatometer tests (SDMT), seismic piezocone tests (SCPTU), boreholes and laboratory tests on samples.

Additional DMTs and CPTUs were performed after construction from the top of the embankment, nearby pre-construction DMTs and CPTUs, in order to detect changes induced in the soil (particularly in stiffness) by the embankment load.

Fig. 1 shows the plan layout of the embankment and the location of all DMT, CPTU, SDMT and SCPTU soundings. Details on DMT results at Treporti are given by Marchetti et al. (2004). Comments on SCPTU and SDMT results are given by McGillivray & Mayne (2004). CPTU results are described by Gottardi & Tonni (2004, 2005). Preliminary laboratory results are presented by Simonini (2004) and Cola & Simonini (2005).

## 4 DMT RESULTS AT TREPOTI

Ten DMT soundings to  $\approx 44-46$  m depth (DMT 11 – DMT 20) were performed at various locations (Fig. 1) before the embankment construction.

C readings were taken every 20 cm, besides A and B readings, to obtain more detailed soil profiles and distinguish layer of different permeability.

A large number of DMTA dissipation tests was carried out to estimate the in situ coefficient of consolidation in the cohesive layers.

Fig. 2 shows the profiles with depth of the main parameters (material index  $I_D$ , constrained modulus  $M$ , undrained shear strength  $c_u$ , horizontal stress index  $K_D$ ) obtained from the interpretation of DMT 14, located at the center of the embankment.

Fig. 3 shows the superimposed profiles of the above parameters obtained from all the ten pre-construction DMT soundings.

Fig. 4 shows the profiles of  $p_0$  and  $p_1$  (corrected A and B readings),  $p_2$  (corrected "closing pressure" C reading), the pore pressure index  $U_D = (p_2 - u_0)/(p_0 - u_0)$  (Lutenegger & Kabir 1988) and the material index  $I_D = (p_1 - u_0)/(p_0 - u_0)$  obtained at the center of the embankment (DMT 14). Details on the use of C readings and  $U_D$  may be found in TC16 (2001).

The DMT investigation indicated the following.

### – Stratigraphic profile

The soil at Treporti, typical of the Venice lagoon, is highly stratified and remarkably heterogeneous. The profiles of  $I_D$  and  $U_D$  indicate that alternating layers of sand, silt and silty clay of variable thickness (rarely  $> 2$  m) are intensely interbedded.

A well-defined layer of sand of significant thickness was found just below the ground surface, in the upper 6-8 m. A thin layer of very soft clay is present at 1.5-2 m depth. The soil between 6-8 m and 20 m

depth is predominantly silt, often interbedded with a variable sand layer between 15 and 18 m.

The "peaks" observed in all  $K_D$  and  $c_u$  profiles, at about 27-28 m, 34-35 m and 43-44 m depths, are due to the presence of thin stiff peat layers.

#### – Stress history and OCR

The OCR- $K_D$  correlation commonly used for clay (Marchetti 1980) indicates that the deposit at Treporti is normally consolidated to slightly overconsolidated ( $K_D \approx 2.5$ , OCR  $\approx 1.2$ -2). These values are in agreement with OCR estimated from oedometer and from observed in situ stress-strain curves (Simonini 2004).

In the upper 6-8 m an overconsolidated "crust" ( $K_D > 5$ -6), maybe due to desiccation, is present.

#### – Constrained modulus $M_{DMT}$

The constrained modulus  $M$  determined from DMT ( $M_{DMT}$ ) is the vertical drained confined (one-dimensional) tangent modulus at  $\sigma'_{vo}$  (same as  $E_{oed} = 1/m_v$  obtained by oedometer). The profiles of  $M_{DMT}$  at Treporti reflect the vertical and horizontal disuniformity of the deposit.  $M_{DMT}$  varies from  $\approx 5$  MPa in soft clay layers to 100-150 MPa in sand layers.

#### – Small strain shear modulus $G_0$

Fig. 5 shows the profiles of the shear wave velocity  $V_S$  obtained from three seismic flat dilatometer tests (SDMT) and three seismic piezocone tests (SCPTU) carried out along the cross section 15–14–19 (see Fig. 1). SDMT and SCPTU tests were performed and interpreted by the Georgia Tech research group (McGillivray & Mayne 2004).

Fig. 6 shows the profiles of the small strain shear modulus  $G_0$  obtained from  $V_S$ , with soil density  $\rho$  estimated from  $\gamma_{DMT}$ .

The profiles of  $G_0$  are more uniform than  $M_{DMT}$ .  $G_0$  increases almost linearly with depth from  $\approx 30$  MPa to  $\approx 150$  MPa at 40 m depth.

#### – Coefficient of consolidation and permeability

Figs. 7 and 8 show the values of the horizontal coefficient of consolidation  $c_h$  (estimated according to Marchetti & Totani 1989) and the horizontal coefficient of permeability  $k_h$  derived from  $c_h$  (Schmertmann 1988, see also TC16 2001) obtained from all DMTA dissipations.

The oscillations in the values of  $c_h$  and  $k_h$  reflect the marked heterogeneity of the deposit. Higher values are influenced by the presence of more permeable silt/sand layers close to the dissipation depths.

The values of  $c_h$  are mostly of the order of  $1 \cdot 10^{-1}$  cm<sup>2</sup>/s. The minimum values of  $k_h$  (in silty clay layers) are higher than usually found in most soft clays. The relatively high values of  $c_h$  obtained from DMTA suggested rather fast primary consolidation, later confirmed by piezometer readings.

Also, the nearly rectilinear shape of the DMTA dissipation curves, in contrast with the usual "S-shape", was interpreted as a likely indicator of significant creep of the soil skeleton and provided a warning that the secondary settlement could be important, as later confirmed by field measurements.

#### – Repetitions of DMTs after construction. Observed variation of DMT results

After completion of the embankment, four DMT soundings to  $\approx 44$  m were performed starting from the top surface of the embankment (Fig. 9), very close ( $\approx 2$  m) to pre-construction DMT soundings.

Fig. 10 shows the profiles of before/after DMT soundings at the center of the embankment. The soil variations due to the embankment load were reflected by the following changes of DMT results:

(a) A reduction in  $K_D$  (i.e. in OCR) is particularly evident in the upper OC crust at 6-8 m depth. This "rejuvenation" is due to the fact that the vertical stress increase in the soil under the embankment load approaches the preconsolidation stress, leading the soil to a nearly NC state.

(b) While  $K_D$  decreased, the dilatometer modulus  $E_D$  increased under the load. Since  $M_{DMT} = f(K_D, E_D)$ , the two opposite variations approximately compensated each other, so that  $M_{DMT}$  remained substantially unchanged. This result, apparently in contradiction with the common notion that  $M$  should increase with stress, can be explained observing that, in oedometer tests,  $M$  stops to increase as the vertical stress  $\sigma'_v$  approaches the preconsolidation pressure  $p'_c$ , or rather, in the case of a pronounced break,  $M$  decreases when  $\sigma'_v$  exceeds  $p'_c$ . It appears fitting that the DMT correlations have indicated no change in modulus, as the tendency of modulus to increase with stress was compensated by the tendency of modulus to decrease nearing the NC state.

(c) A slight increase in  $c_u$ , more evident in the soft clay layer at 1.5-2 m below the ground surface.

(d) An increase in  $\sigma'_h = K_0 \sigma'_v$  with  $K_0$  estimated from DMT in clay, similar to the corresponding  $\Delta\sigma_h$  calculated by Boussinesq. This is a broad confirmation of the DMT  $K_0$  correlation for clay.

## 5 OBSERVED PORE PRESSURES AND DEFORMATIONS

The monitoring instrumentation installed at Treporti and the field measurement results are described in detail by Simonini (2004). The most significant indications obtained by field measurements are summarized here below.

#### – Pore pressures during/after construction

Piezometer readings indicated no detectable excess pore pressure due to consolidation in any layer

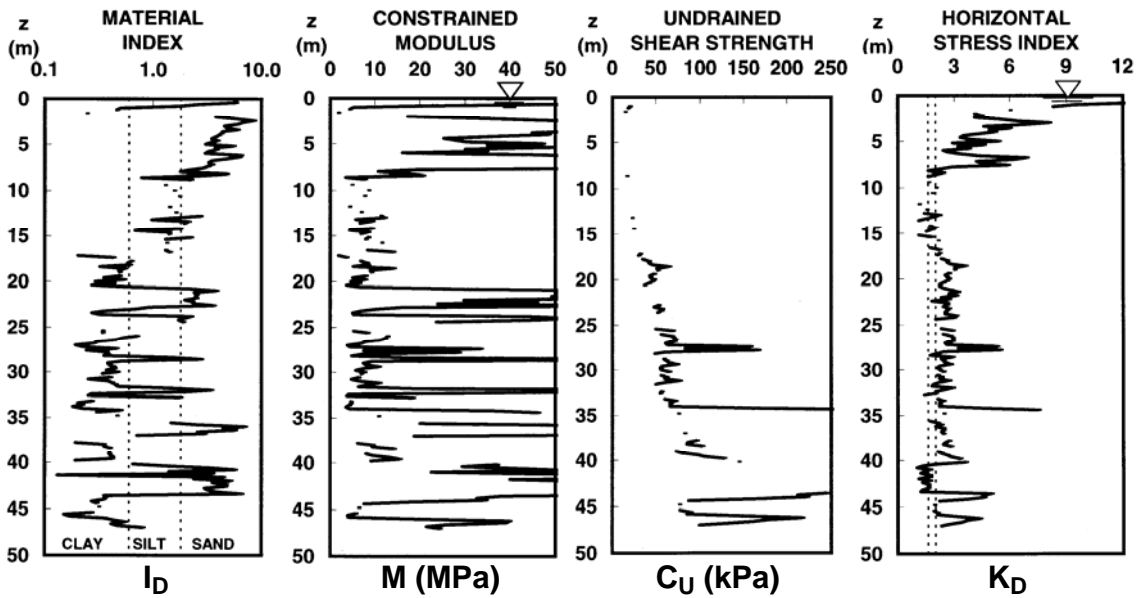


Fig. 2. DMT profiles at the center of the embankment (DMT 14)

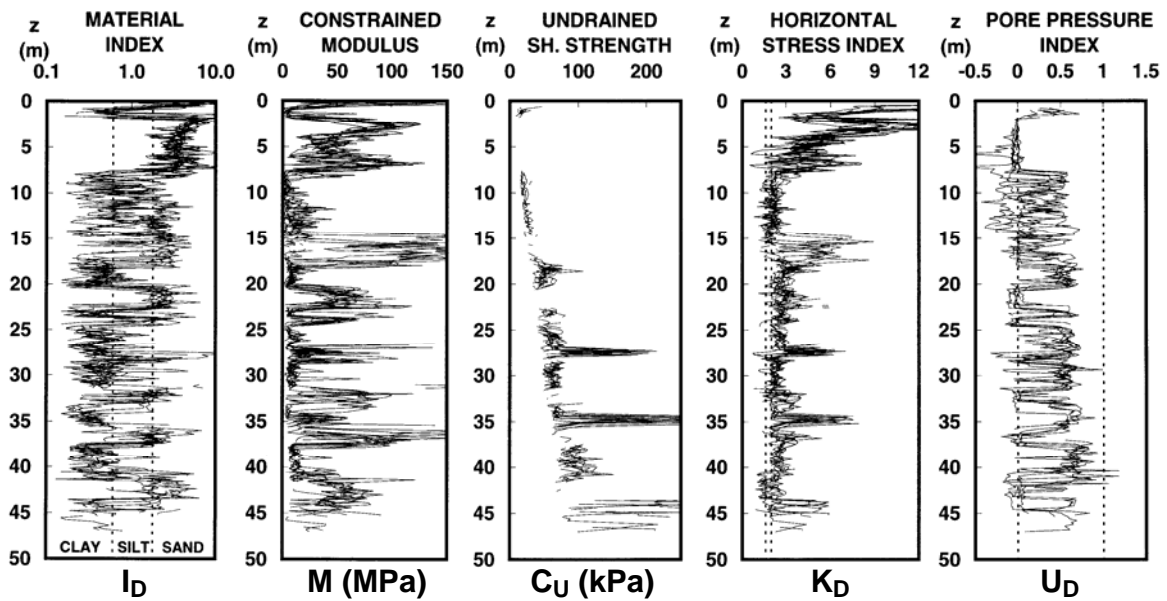


Fig. 3. Superimposed profiles of all DMT soundings (DMT 11, 12, ..., 20)

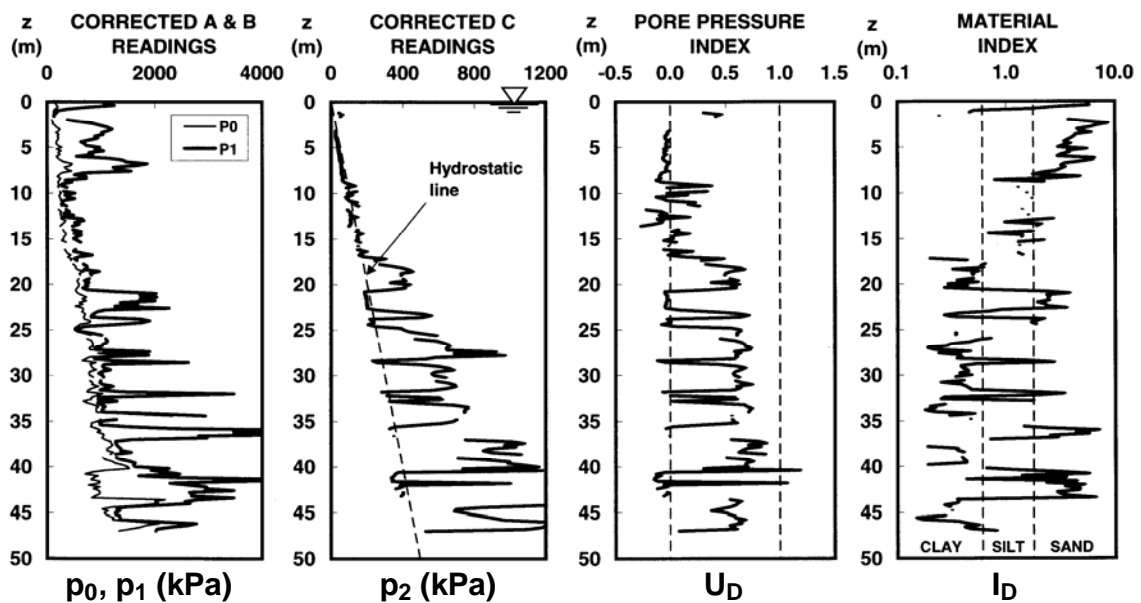


Fig. 4. Profiles of  $p_0$  &  $p_1$ ,  $p_2$ ,  $U_D$  and  $I_D$  at the center of the embankment (DMT 14)

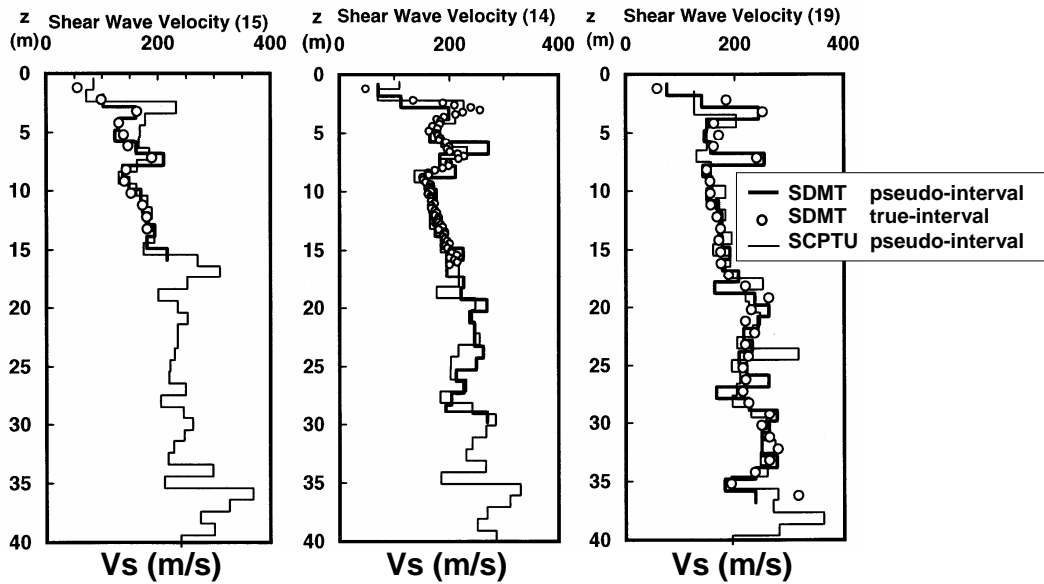


Fig. 5. Profiles of shear wave velocity  $V_S$  along the cross section 15–14–19

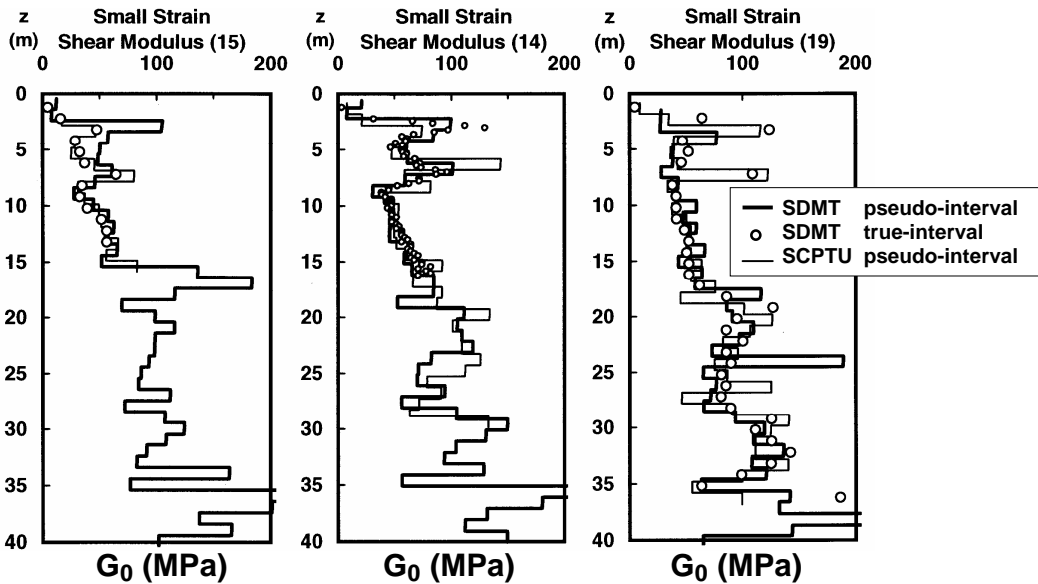


Fig. 6. Profiles of small strain shear modulus  $G_0$  along the cross section 15–14–19

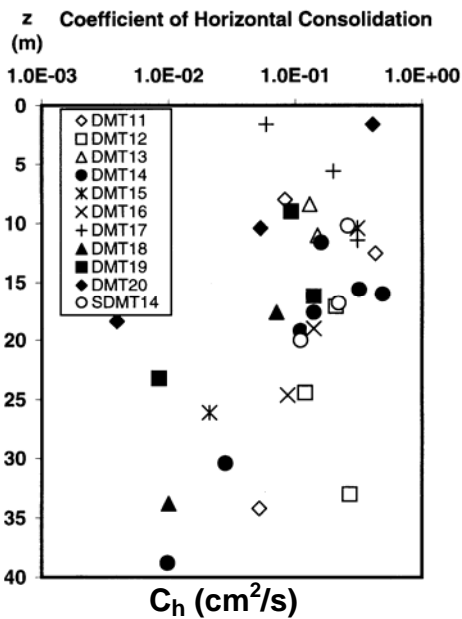


Fig. 7. Coefficient of horizontal consolidation

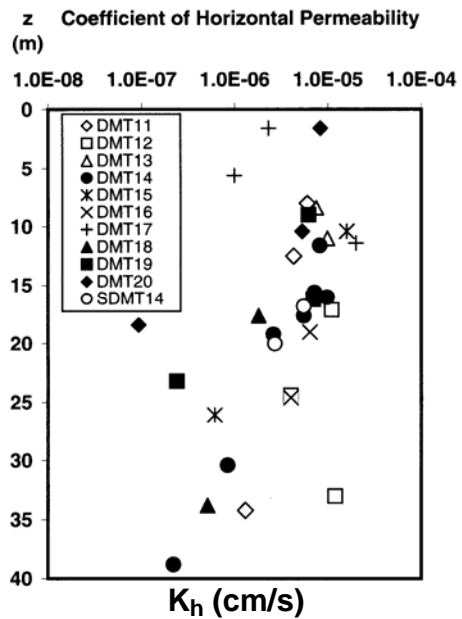


Fig. 8. Coefficient of horizontal permeability



Fig. 9. Positioning of the penetrometer truck for testing after embankment construction

during and after the embankment construction (fully drained conditions throughout).

Due to the high drainage properties of the soils, primary consolidation was rather fast and contemporary with the six-month embankment construction.

– *Settlement-time curve*

Fig. 11 shows the evolution with time of the total settlement measured at the center of the embankment, during and after construction.

The total settlement measured under the center the day of embankment completion, i.e. 180 days after the beginning of construction, was  $\approx 36$  cm. This settlement includes, besides immediate and primary, also the secondary settlement developed in the 180 days of construction, occurred essentially in drained conditions.

Secondary during construction was presumably significant. On 2 September 2004, i.e. 540 days after the end of construction (last reading available to the writers), the total measured settlement was  $\approx 48$  cm,

hence an additional secondary settlement of  $\approx 12$  cm developed under constant load.

Note that the after-construction secondary settlement alone is about 25 % of the total settlement measured so far.

As remarked by Cola & Simonini (2005), secondary settlements play a key role in the overall time-dependent response of the relatively free draining, predominantly silty Venice lagoon soils. It is difficult to clearly distinguish between the primary and secondary compression, the latter seeming to occur from the very beginning of the compression phase. Consequently, the interpretation of the settlement-time curve, by use of the classic primary-followed-by-secondary model, is not straightforward.

Cola & Simonini (2005) also present values of the secondary compression index  $C_{\alpha}$  obtained from laboratory and from interpretation of the full-scale strain-time curves observed at Treporti (Fig. 12).

– *Local vertical strains*

Measurements of local vertical strains at 1 m depth intervals, down to 57 m depth, were obtained by use of high-accuracy multiple extensometers (sliding micrometers).

Fig. 13a shows the distribution with depth of local vertical strains  $\epsilon_v$  measured at the center of the embankment under various loads throughout the embankment construction (in 180 days) and 540 days after the end of construction, under constant load. The corresponding accumulated settlements  $S$  are shown in Fig. 13b.

Fig. 13 clearly shows that vertical strains and settlements are mostly concentrated in the shallow soft clay layer at 1.5-2 m depth and in the silt layer between  $\approx 8$  and 20 m depth. The maximum vertical strain  $\epsilon_v$  measured in these layers at the end of construction is about 3 to 5 %. The contribution of soil layers deeper than 35-40 m appears negligible.

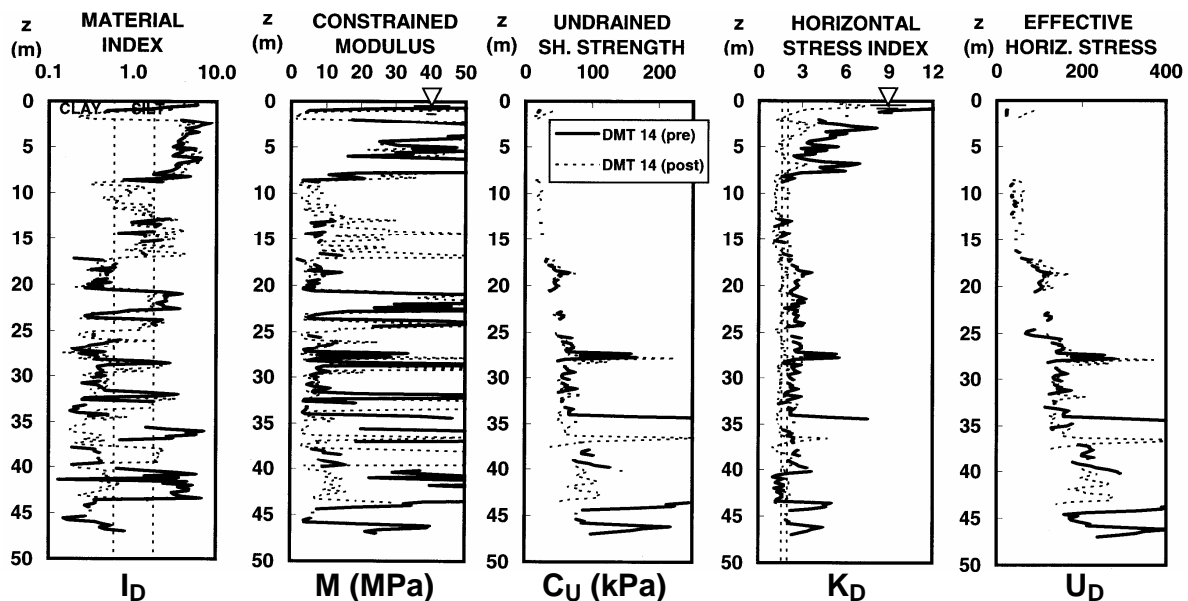


Fig. 10. DMT profiles before/after construction at the center of embankment (DMT 14)

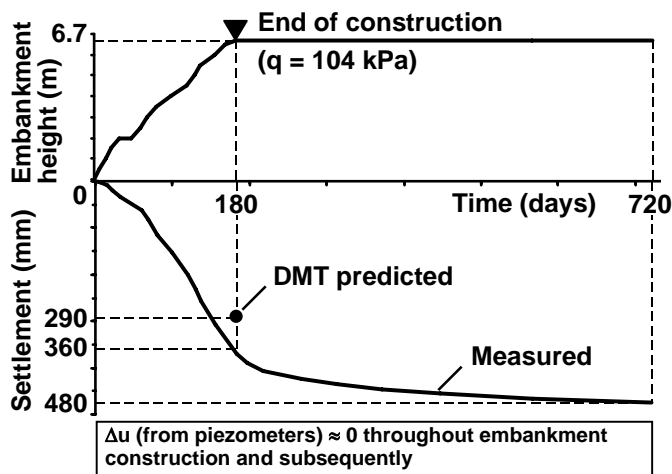


Fig. 11. Settlement-time curve at the center of the embankment and comparison of settlements predicted by DMT and measured at the end of construction

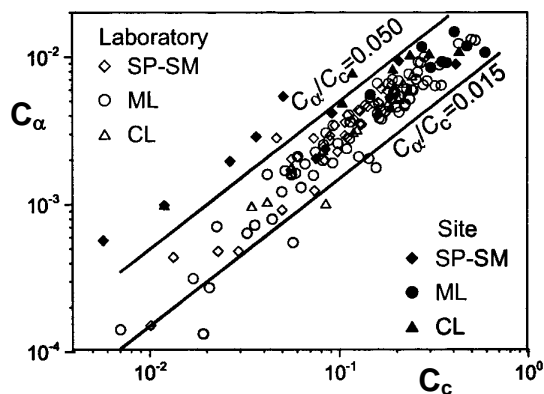


Fig. 12. Ratio between secondary and primary compression indexes  $C_\alpha/C_c$  obtained from laboratory and from observed full-scale strain-time curves (Cola & Simonini 2005)

– Horizontal vs vertical deformations

The comparison of vertical and horizontal displacements, measured by inclinometers (Fig. 14), indicated that the total vertical displacement is one order of magnitude greater than the maximum horizontal displacement, i.e. soil compression occurred mostly in the vertical direction, as also shown in Fig. 15.

6 COMPARISON OF DMT-PREDICTED VS OBSERVED SETTLEMENTS

Settlements were predicted by DMT, before the field results were available, by use of the classic 1-D formula  $S = \Sigma (\Delta\sigma_v/M) \Delta z$ , assuming  $M = M_{DMT}$ . Vertical stress increments  $\Delta\sigma_v$  were calculated by current linear elasticity solutions for a circular uniform surface load (Poulos & Davies 1974). Details on settlement calculation by DMT at Treporti can be found in Marchetti et al. (2004).

As remarked in TC16 (2001), the settlements calculated by DMT according to the above expression are *primary consolidation* settlements (i.e. net of immediate and secondary). To obtain the total values, the immediate and secondary settlements need to be added.

DMT predicted a primary settlement of 267 mm at the center of the embankment, 101 to 160 mm at the edge. The immediate (undrained) settlement of the sole clay layers at the center of the embankment was estimated as  $\approx 20$ -23 mm. Hence the settlement predicted by DMT at the end of construction, net of secondary developed during construction (DMT does not predict secondary), was 29 cm.

The DMT-predicted 29 cm is 7 cm less (20 % less) than the 36 cm measured at the end of

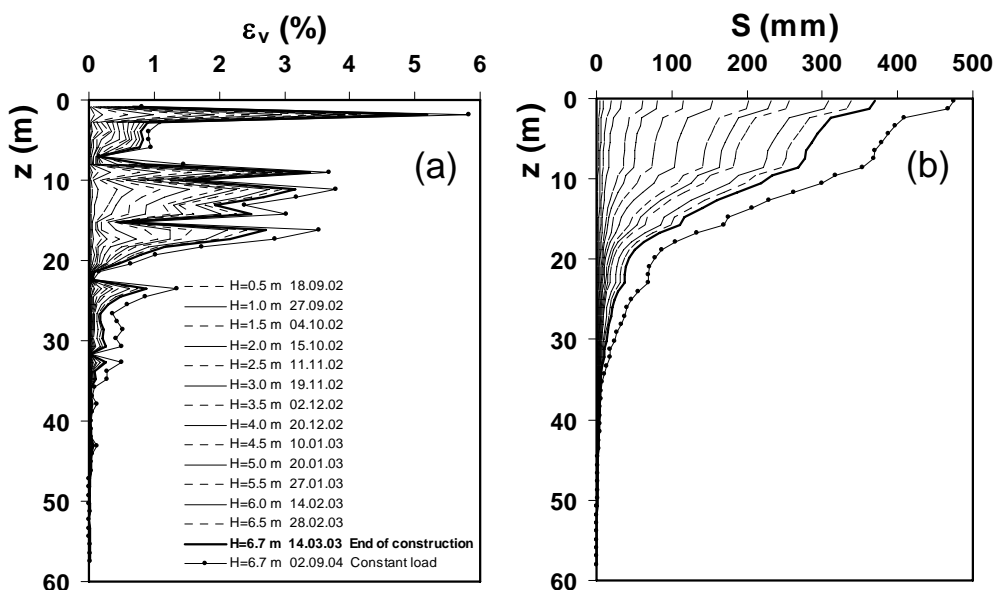


Fig. 13. (a) Vertical strains measured every 1 m depth under the center of the embankment and (b) corresponding accumulated settlements (updated after Simonini 2004)

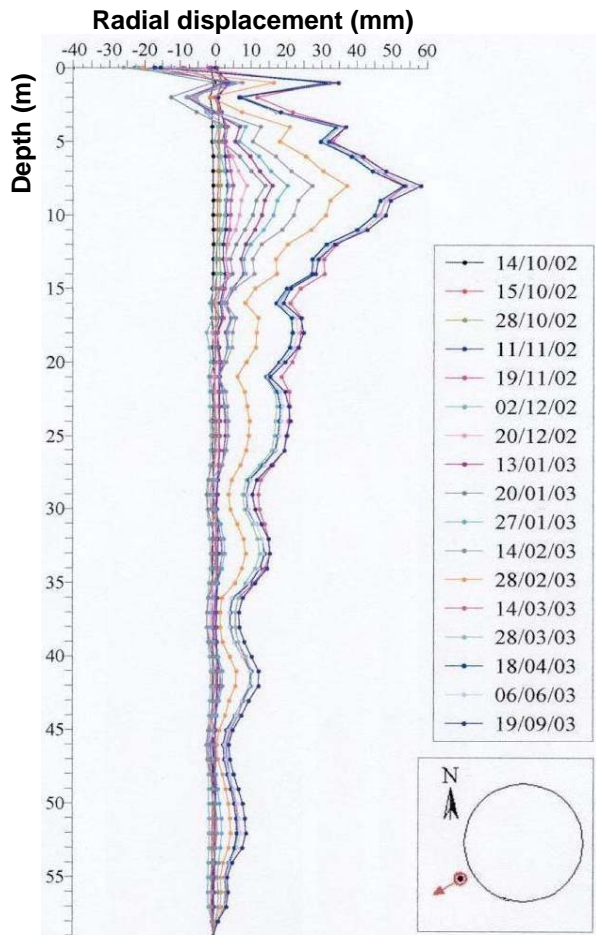


Fig. 14. Radial displacement measured by inclinometer at the edge of the embankment

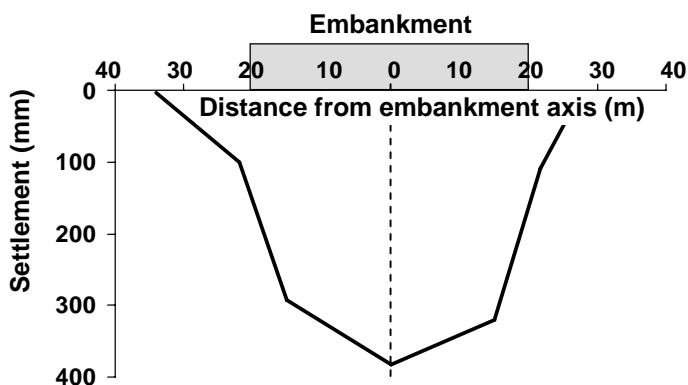


Fig. 15. Settlement profile measured at the end of construction across the embankment cross section SW-NE

construction (Fig. 11). However, if homologous quantities have to be compared, the 36 cm developed during the 180 days of construction should be reduced of the contribution of the secondary during construction. Quantifying such contribution would require a specific analysis separating primary from secondary. Such deduction, however, should end up not very different from the above mentioned difference. If this view is correct, the ability of DMT to predict settlement (net of secondary) proved in this case quite satisfactory.

## 7 COMPARISON OF $M$ BY DMT AND $M$ BACKCALCULATED FROM MEASURED LOCAL VERTICAL STRAINS

Fig. 16a shows the comparison of the profiles of the 1-D constrained moduli  $M_{DMT}$  obtained by DMT 14 and  $M$  backcalculated from local vertical strains measured every 1 m depth by the sliding micrometer located at the center of the embankment, at the end of construction.

$M$  values were backcalculated from local vertical strains  $\Delta\varepsilon_v$  measured in each 1 m soil layer as  $M = \Delta\sigma_v / \Delta\varepsilon_v$ , with vertical stress increments  $\Delta\sigma_v$  calculated at the mid-height of each layer by linear elasticity formulae (approximation considered acceptable in view of the very low  $\varepsilon_h$  as in Figs. 14 and 15).

The comparison in Fig. 16a shows that the profile of  $M_{DMT}$  (values obtained every 0.2 m depth) is much more variable than the profile of  $M$  backfigured from measurements. This was expectable, since  $M$ -backfigured is an "average" over 1 m.

In Fig. 16b the profile of the local vertical strains  $\Delta\varepsilon_v$  measured by the sliding micrometer at the center of the embankment, at the end of construction, is compared to the profile of  $\Delta\varepsilon_v$  calculated by  $M_{DMT}$  (from DMT 14) as  $\Delta\varepsilon_v = \Delta\sigma_v / M_{DMT}$ . The corresponding profiles of measured and DMT-calculated settlements  $S$  are compared in Fig. 16c.

Note that the vertical strains/settlements calculated by  $M_{DMT}$ , shown in Figs. 16b and c, are due solely to primary consolidation (net of immediate and secondary), while the measured values also include immediate and secondary during construction.

Fig. 16b shows that  $M_{DMT}$  slightly underestimates the vertical strains in the upper 15-20 m and slightly overestimates them below this depth. However, these errors partially compensate each other when the local vertical strains are summed up to obtain the accumulated settlement (Fig. 16c).

The comparisons in Fig. 16 indicate an overall satisfactory agreement between  $M_{DMT}$  and  $M$  backcalculated at the end of construction.

## 8 IN SITU DECAY CURVES OF SOIL STIFFNESS WITH STRAIN LEVEL

The comparisons in the previous section indicate an overall satisfactory ability of  $M_{DMT}$  to predict the observed  $M$  – under the fully applied load.

As a subsequent step,  $M_{DMT}$  (one value at a given depth) was compared with the (variable, dependent on the applied load) moduli backcalculated at various stages during construction.

As shown in this section (where the analyses are carried out in terms of Young's modulus  $E$ ), moduli backfigured at small fractions of the final load were much higher than final moduli.



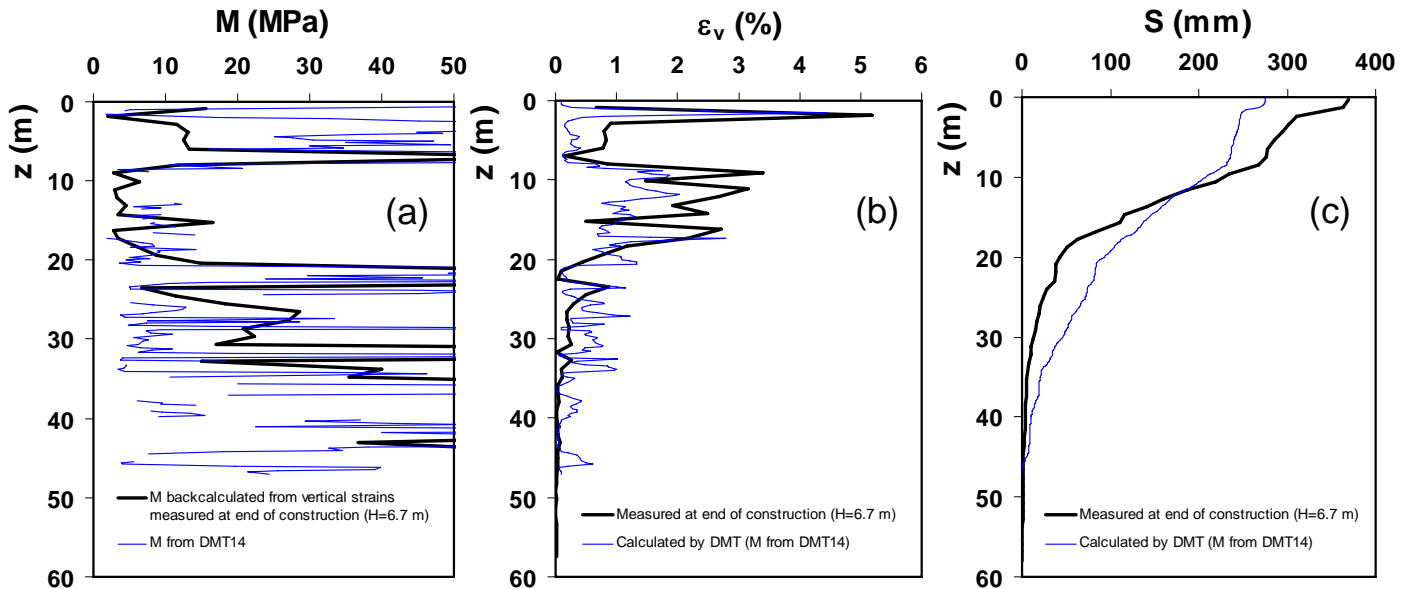


Fig. 16. Comparison of (a)  $M_{DMT}$  vs  $M$  backcalculated from measurements, (b) vertical strains  $\varepsilon_v$  and (c) accumulated settlement  $S$  measured under the center of the embankment at the end of construction and calculated by  $M_{DMT}$

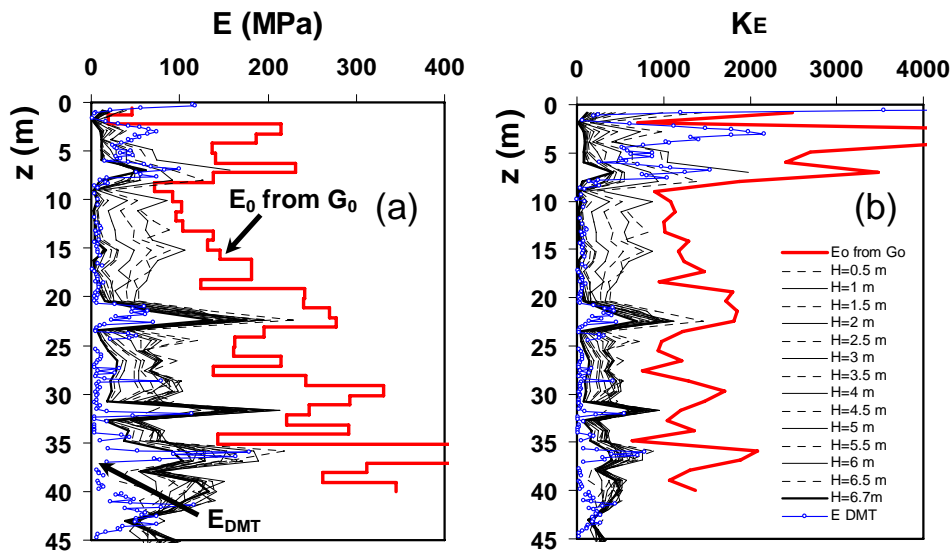


Fig. 17. Variation of (a) secant Young's modulus  $E$  backcalculated from vertical strains measured under the center of the embankment under various loads throughout embankment construction and (b) corresponding modulus number  $K_E$

Fig. 17a shows the variation of secant Young's moduli  $E$  backcalculated from local vertical strains measured at 1 m depth intervals by the sliding micrometer located at the center of the embankment, under each load increment ( $\Delta q \approx 8$  kPa for each 0.50 m thick added sand layer), from the beginning to the end of construction.

The moduli  $E$  were calculated at the mid-height of each 1 m soil layer based on linear elasticity formulae. The vertical and radial stress distributions  $\Delta\sigma_v$  and  $\Delta\sigma_r$  under each load increment were calculated according to current linear elasticity solutions (Poulos & Davies 1974), assuming a Poisson's ratio  $\nu = 0.15$ .

$E$  values backcalculated at depths greater than 35-40 m may not be dependable, due to the very small measured deformations. Also, a few anomalous "peaks" in the  $E$  profiles, derived from uncertain

values of strains locally measured under the small initial loads, have been ignored.

The profile of the small strain Young's modulus  $E_0$  (initial modulus) is also shown in Fig. 17a.  $E_0$  was derived from  $G_0$  obtained from  $V_s$  measured at the center of the embankment (SCPTU 14) via elasticity theory, assuming  $\nu = 0.15$ .

Fig. 17a shows the progressive reduction of the backcalculated moduli  $E$  under increasing load. Such variation of soil moduli should reflect the combined effects – of opposite sign – of the increase in stress and strain level (stiffness should increase with stress and decrease with strain).

In order to separate the two effects, the dependence of  $E$  on current stress level was taken into account, as a first approximation, by use of the classic Janbu's relation  $E = K_E p_a (\sigma'_v / p_a)^n$ , where  $K_E$  = modulus number,  $p_a$  = reference atmospheric

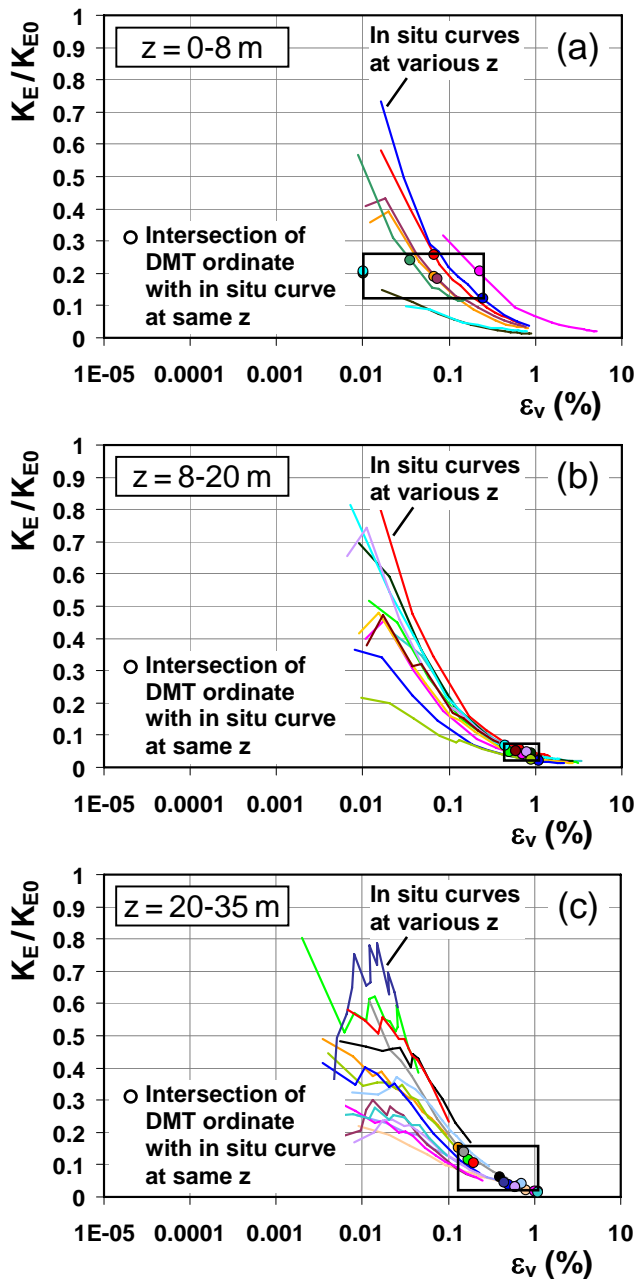


Fig. 18. Curves of decay of soil stiffness with vertical strain backcalculated from measurements (curves labeled "In situ curves") and their intersection with datapoints corresponding to DMT moduli  $M_{DMT}$  at the same depth

pressure (100 kPa) and  $\sigma'_v =$  current vertical effective stress. The exponent  $n$  was assumed = 0.8, from back-fitting of the observed moduli profiles.

Fig. 17b shows the variation of the modulus number  $K_E$  corresponding to the  $E$  values backcalculated under each load increment. Fig. 17b clearly shows the decay of soil stiffness with increasing strain level, even purged of the effects of stress increase.

In situ curves of decay of soil stiffness with strain level were reconstructed, at 1 m depth intervals, from local vertical strains measured at the center of the embankment under each load increment, from the very small initial loads up to the final load of 104 kPa.

In order to account for the effect of varying stress level on the backcalculated moduli, these curves, shown in Fig. 18, are expressed in terms of variation of the ratio of the modulus number  $K_E$  corresponding to the backcalculated  $E$  values to the modulus number  $K_{E0}$  corresponding to the initial modulus  $E_0$ , obtained by Janbu's expression for  $E=E_0$  and  $\sigma'_v=\sigma'_{v0}$ .

The sets of curves shown in Fig. 18 are representative of different soil layers: (a) the upper sand layer (depth  $z = 0$  to 8 m), (b) the intermediate silt layer ( $z = 8$  to 20 m) – which gave rise to most of the observed settlements, and (c) the silty-sandy layers between  $z = 20$  to 35 m.

As shown in Fig. 18, the smallest detectable values of vertical strains  $\epsilon_v$  measured by the sliding micrometer are in the range  $\approx 0.5-1 \cdot 10^{-2}$  %. Therefore the initial part of the curves, at very small to small strains, is missing.

Research currently in progress investigates the possible use of the seismic dilatometer (SDMT) for deriving in situ decay curves of soil stiffness with strain level ( $G-\gamma$  curves or similar). Such curves could be tentatively constructed by fitting "reference typical-shape" laboratory curves through two points, both obtained by SDMT: (1) the initial shear modulus  $G_0$  from  $V_S$ , and (2) a modulus at "operative" strains, corresponding to  $M_{DMT}$  – provided the strain range corresponding to  $M_{DMT}$  is defined.

Preliminary indications (Mayne 2001, Ishihara 2001) have suggested that the shear strain range corresponding to  $M_{DMT}$  is  $\approx 0.05-0.1\%$  to 1 %.

To investigate this point, datapoints corresponding to DMT moduli have been superimposed to the observed in situ decay curves in Fig. 18. The rectangular areas in Fig. 18 represent, at each depth interval, the range of values of the ratio  $K_E/K_{E0}$  corresponding to  $E_{DMT}/E_0$ , where  $E_{DMT}$  is the Young's modulus derived from the constrained modulus  $M_{DMT}$  (DMT 14) via elasticity theory, for  $\nu = 0.15$ . The values of  $E_{DMT}$  were obtained as average values over 1 m soil layers at each measurement depth.

The comparison of DMT datapoints with the observed in situ decay curves in Fig. 18 indicates that the moduli estimated from DMT ( $M_{DMT}$ ) are located in a range of vertical strains  $\epsilon_v \approx 0.1$  to 1 %, 0.5% on average, a result that agrees with the preliminary indications (Mayne 2001, Ishihara 2001).

A note of caution: The vertical strain ( $\epsilon_v$  in the abscissas of Fig. 18) appears a legitimate substitute of the shear strain  $\gamma$ , given the "negligible" values of  $\epsilon_h$  (it is reminded that  $\gamma_{max} = \epsilon_1 - \epsilon_3$ ). Hence the decay curves in Fig. 18 could be regarded as common curves of moduli decay with shear strains.

However the oedometer-like pattern of deformation of the loaded soil (Figs. 14 and 15) would induce to expect an increase – not a decrease – of the modulus with the applied load (as in the oedometer), unless the applied load exceeds the preconsolidation stress, which is probably the case for the studied site.

Then the decreasing trends in Fig. 18 could be due to the combined effect of the two mentioned causes.

## 9 CONCLUSIONS

A full-scale instrumented test embankment (40 m in diameter, 6.70 m high, applied load 104 kPa) was built at the site of Treporti, typical of the silty deposits in the Venice lagoon area.

The most significant results obtained from comparison of DMT results with the in situ observed embankment behavior, presented in this paper, are:

(a) The settlement predicted by DMT at the end of construction (net of secondary developed during construction) is in good agreement with the measured settlement.

(b) The comparison of the profiles of moduli  $M$  obtained from DMT and backcalculated from local vertical strains measured every 1 m depth under the center of the embankment, at the end of construction, shows an overall satisfactory agreement.

(c) Field measurements show a progressive reduction of the backcalculated moduli  $E$  with increasing strain level. In situ full-scale curves of decay of soil stiffness with strain level were reconstructed from local vertical strains measured at the center of the embankment, at 1 m depth intervals, under each load increment throughout the embankment construction. From comparison with the observed in situ decay curves, the moduli estimated from DMT are located in the strain range  $\varepsilon_v \approx 0.1$  to 1%, 0.5% on average. This finding may help for the development of methods for deriving in situ decay curves of soil stiffness with strain level from seismic dilatometer (SDMT).

## ACKNOWLEDGMENTS

The authors wish to thank for their cooperation P.W. Mayne, Alec McGillivray and the Georgia Tech research group (Atlanta, USA), the Universities of Padova and Bologna (Italy), the Soil Test company (Arezzo, Italy).

This study was funded by the Italian Ministry of University and Scientific Research.

The technical and financial support of Consorzio Venezia Nuova is also acknowledged.

## REFERENCES

- Cola, S. & Simonini, P. 2005. Relevance of secondary compression in Venice lagoon silts. *Proc. XVI ICSMGE, Osaka*, Vol. 2, 491-494.
- Gottardi, G. & Tonni, L. 2004. Use of piezocone tests to characterize the silty soils of the Venetian lagoon (Treporti test site). *Proc. 2<sup>nd</sup> Int. Conf. on Site Characterization ISC'2, Porto*, Vol. 2, 1643-1650.
- Gottardi, G. & Tonni, L. 2005. The Treporti test site: Exploring the behaviour of the silty soils of the Venetian lagoon. *Proc. XVI ICSMGE, Osaka*, Vol. 2, 1037-1040.
- Ishihara, K. 2001. Estimate of relative density from in-situ penetration tests. *Proc. Int. Conf. on In Situ Measurement of Soil Properties and Case Histories, Bali*, 17-26.
- Lutenegger, A.J. & Kabir, M.G. 1988. Dilatometer C-reading to help determine stratigraphy. *Proc. ISOPT-1, Orlando*, Vol. 1, 549-554.
- Marchetti, S. 1980. In Situ Tests by Flat Dilatometer. *ASCE Jnl GED*, 106, GT3, 299-321.
- Marchetti, S., Monaco, P., Calabrese, M. & Totani, G. 2004. DMT-predicted vs measured settlements under a full-scale instrumented embankment at Treporti (Venice, Italy). *Proc. 2<sup>nd</sup> Int. Conf. on Site Characterization ISC'2, Porto*, Vol. 2, 1511-1518.
- Marchetti, S. & Totani, G. 1989. Ch Evaluations from DMTA Dissipation Curves. *Proc. XII ICSMFE, Rio de Janeiro*, Vol. 1, 281-286.
- Mayne, P.W. 2001. Stress-strain-strength-flow parameters from enhanced in-situ tests. *Proc. Int. Conf. on In Situ Measurement of Soil Properties and Case Histories, Bali*, 27-47.
- McGillivray, A. & Mayne, P.W. 2004. Seismic piezocone and seismic flat dilatometer tests at Treporti. *Proc. 2<sup>nd</sup> Int. Conf. on Site Characterization ISC'2, Porto*, Vol. 2, 1695-1700.
- Poulos, H.G. & Davis, E.H. 1974. Elastic Solutions for Soil and Rock Mechanics. John Wiley & Sons.
- Ricceri, G. & Butterfield, R. 1974. An analysis of compressibility data from a deep borehole in Venice. *Géotechnique* 24(2), 175-192.
- Schmertmann, J.H. 1988. Guidelines for Using the CPT, CPTU and Marchetti DMT for Geotechnical Design. Rept. No. FHWA-PA-87-022+84-24 to PennDOT, Office of Research and Special Studies, Harrisburg, PA.
- Simonini, P. 2004. Characterization of the Venice lagoon silts from in-situ tests and the performance of a test embankment. *Proc. 2<sup>nd</sup> Int. Conf. on Site Characterization ISC'2, Porto*, Vol. 1, 187-207.
- TC16 - Marchetti, S., Monaco, P., Totani, G. & Calabrese, M. 2001. The Flat Dilatometer Test (DMT) in Soil Investigations - A Report by the ISSMGE Committee TC16. *Proc. Int. Conf. on In Situ Measurement of Soil Properties and Case Histories, Bali*, 95-131.